Received: 25 March 2020 | Revised: 21 July 2020 | Accepted: 22 July 2020
DOI: 10.1002/aoc.5962

FULL PAPER

Applied Organometallic Chemistry WILEY

Synthesis of Novel Triazole Incorporated Thiazolone Motifs Having Promising Antityrosinase Activity through Green Nanocatalyst CuI-Fe_3O_4@SiO_2 (TMS-EDTA)

Mahdieh Darroudi[1] | Sara Ranjbar[2] | Mohammad Esfandiar[1] | Mahsima Khoshneviszadeh[3] | Mahshid Hamzehloueian[4] | Mehdi Khoshneviszadeh[3,5] | Yaghoub Sarrafi[1]

[1]Department of Organic Chemistry, Faculty of Chemistry, University of Mazandaran, Babolsar, 47416, Iran
[2]Pharmaceutical Sciences Research Center, Shiraz University of Medical Sciences, Shiraz, Iran
[3]Medicinal and Natural Products Chemistry Research Center, Shiraz University of Medical Sciences, Shiraz, Iran
[4]Department of Chemistry, Jouybar Branch, Islamic Azad University, Jouybar, Iran
[5]Department of Medicinal Chemistry, School of Pharmacy, Shiraz University of Medical Sciences, Shiraz, Iran

Correspondence
Mehdi Khoshneviszadeh, Department of Medicinal Chemistry, School of Pharmacy, Shiraz University of Medical Sciences, Shiraz, Iran.
Email: khoshnevim@sums.ac.ir

Yaghoub Sarrafi, Department of Organic Chemistry, Faculty of Chemistry, University of Mazandaran, 47416 Babolsar, Iran.
Email: ysarrafi@umz.ac.ir

In the present work, novel 5-((1-benzyl-1,2,3-triazol-4-yl)methoxybenzylidene)-2-(arylamino)thiazol-4-one thiazolone incorporated triazole derivatives have been designed as tyrosinase inhibitors. The compounds were synthesized through click reaction in good yield. Moreover, the antityrosinas activity of the synthesized derivatives was evaluated. In the search for establishing a click copper-catalyzed azide/alkyne cycloaddition (CuAAC) reaction under strict conditions, in terms of a novel air-stable, a recyclable and efficient magnetic catalyst was planned for new triazole derivatives as a well-organized copper iodide supported on the functionalized Fe_3O_4@SiO_2 core-shell (CuI/Fe_3O_4@SiO_2 (TMS-EDTA) nanoparticles). The engineered nanocatalyst synthesized for the first time and characterized by different methods, including FT-IR spectroscopy, XRD, FESEM, EDX, TEM, TGA, and BET analysis. The excellent catalytic performance in ethanol with high surface area (351.7 m^2g^{-1}) and short reaction time for diverse functional groups (120–200 min), no use of toxic solvents, reusability of the catalyst, and using eco-friendly conditions are the advantageous of this work. Moreover,the nanocatalyst can be used at least five times without any significant decrease in the yield of the reaction. The thiazolidine-triazole derivatives **9a**, **9c**, **9e**, and **9 g** showed promising tyrosinase inhibitory activity with IC_{50} values in the range of 5.90–9.81 μM. The compounds were found to be considerably more potent tyrosinase inhibitors than the reference inhibitor kojic acid (IC_{50} = 18.36 μM).

KEYWORDS
click reaction, magnetic nanoparticle catalyst, novel Thiazolone-triazole, Tyrosinase inhibitor

1 | INTRODUCTION

1,2,3–Triazole and thiazolone scaffolds have shown various biological activities including; antitumors,[1,2] anti-HIV,[3] anti-allergy,[4] antifungal,[5–7] anti-infection,[8,9] anticancer,[10] antiviral,[11–13] and antimicrobial properties.[14–22] Furthermore, the regioselectivity of cycloadducts is crucial[23–26] and it has been found that some 1,2,3-triazole and thiazolone derivatives exhibited antityrosinase activity.[23–26] Tyrosinase, also known as polyphenol oxidase, is a copper-containing enzyme abundantly distributed in nature. This enzyme participates in the biosynthesis of melanin by catalyzing the hydroxylation of L-tyrosine to 3,4-dihydroxyphenylalanine, L-DOPA (mycophenolate activity) and subsequently, oxidation of L-DOPA to dopaquinone (diphenolase activity).[27] Tyrosinase inhibitors are beneficial for the treatment of hyperpigmentation and neurodegenerative disorders.[28,29] In addition, tyrosinase plays an important role in the oxidation of vegetables and fruits phenolic compounds; hence, some tyrosinase inhibitors have been applied in the food industry as effective anti-browning agents preventing fruits and vegetable deterioration.[30]

One of the most effective synthetic tools for the convenient preparation of hybrid structures of biologically active scaffolds is the click reaction between an azide and a terminal alkyne.[31,32] Accordingly, copper-catalyzed azide/alkyne cycloaddition (CuAAC) reaction is known as a utilized, reliable, and straightforward way for triazole cycloadducts production (Scheme 1).[33–42] Until now, different copper-containing catalysts such as $CuSO_4$,[43,44] CuI,[45,46] Cu_2O, $CuFe_2O_4$ nanoparticles,[47] Cu/C, Cu/SiO_2,[48–50] and polymer capped Cu/Cu_2O[49] have been used for the click reaction. Generally, Cu(I) salt or in situ reductions of Cu (II) can be used as a homogenous catalyst for the regioselective CuAAC reactions.[45,48,50–53] However, homogeneous copper catalysts have some problems, such as not-recyclability, inconvenient separation, and environmental pollution.[54] Through immobilization of copper, two-goal lines are achieved, a) stabilization of copper species, b) preparation of a new heterogeneous catalyst for novel thiazolone-triazole scaffolds synthesis *via* click reaction under green conditions. Among various supporting materials being used for nanoparticles, the use of functionalized magnetic nanoparticles (Fe_3O_4) has attracted much attention to the chemical community. The magnetic nanoparticle offers unique advantages making this support as a more sustainable catalyst including readily available support with high surface area, immobilization of metals and ligands, easy preparation, adsorption, and also easy separation from the reaction mixture through an external magnet.[55–62] The core-shell supported CuI nanoparticles with high specific surface area, small sizes, and reusability are being used as click catalysts to improve the efficiency of the triazoles synthesis.[63–71]

In this study, based on the antityrosinase effect of the thiazolone and triazole heterocycles, the thiazolone-triazole hybrid scaffold was designed. The 5-((1-benzyl-1,2,3-triazol-4-yl)methoxybenzylidene)-2-(arylamino) thiazol-4-one derivatives were synthesized *via* efficient and simple CuAAC reactions. These 1,2,3-triazoles were prepared in the presence of an $CuI/Fe_3O_4@SiO_2$(TMS-EDTA) nanoparticles as an efficient and recyclable magnetic catalyst in ethanol at high yields while having very short reaction time. It is pivotal to point out that, at the end of the reaction, the catalyst was separated with a simple method and reused in further reactions without any significant catalytic activity loss. Finally the synthesized compounds were evaluated for their inhibitory effect on the diphenolase activity of mushroom tyrosinase enzyme.

2 | EXPERIMENTAL

2.1 | Materials and instruments

All the chemicals were purchased from Merck and Sigma-Aldrich. The reactions were monitored by thin layer chromatography (TLC). Melting points were measured on an Electrothermal 9,100 apparatus. NMR spectra were recorded with a Bruker DRX-400 AVANCE instrument (400.1 MHz for ^1H, 100.6 MHz for ^{13}C) with $CDCl_3$ as a solvent. IR spectra were recorded on an FT-IR Bruker vector 22 spectrometers. Mass spectra were recorded on a Finnigan-Matt 8,430 mass spectrometer operating at an ionization potential of 70 eV in Babolsar.

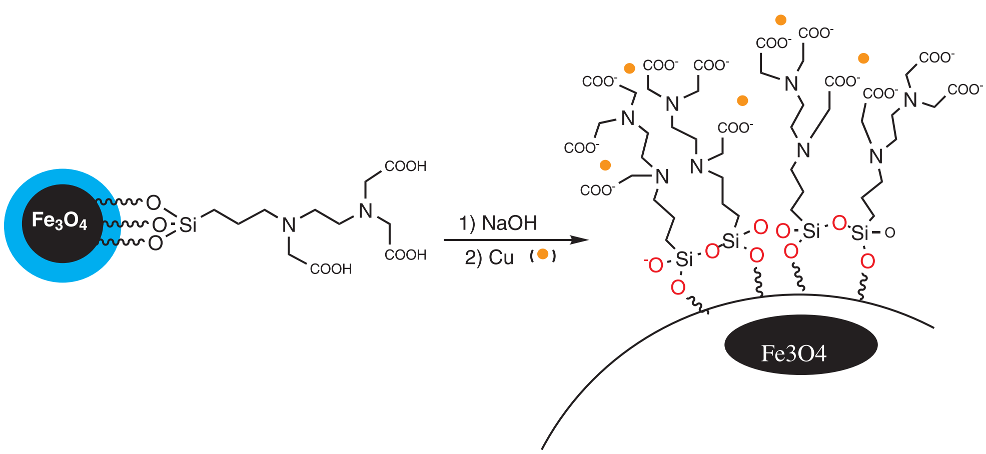

SCHEME 1 Preparation of $Cu/Fe_3O_4@SiO_2$(TMS-EDTA)

Elemental analyses were carried with a Perkin-Elmer 2400II CHNS/O Elemental Analyzer. X-ray diffraction (XRD) patterns were recorded on a Philips PW1730 diffractometer using Cu Kα radiation of wavelength 1.54056 A°. Field Emmision Sanning Electron Microscopy (FESEM) was recorded using a Tescan MIRA III. Thermogravimetric analysis (TGA) and differential thermal analysis (DTA) were recorded on a Q600 (TA, USA) in Tehran and Kashan.

2.2 | Preparation and characterization of copper iodide $Fe_3O_4@SiO_2$ (TMS-EDTA)

The $Fe_3O_4@SiO_2$ (TMS-EDTA) nanoparticle was prepared according to the literature.[72–76] Afterward, the resulting $Fe_3O_4@SiO_2$ (TMS-EDTA) nanoparticle was dispersed in copper (II) sulfate solution (1 M, 25 ml in deionized water) and stirred at 60 °C for 15 hr. The resulting hybrid was separated with a magnet and washed successively with water (3 × 10 mL) and finally dried in vacuum at room temperature to give the CuI supported-$Fe_3O_4@SiO_2$ (TMS-EDTA) nanoparticles. Consequently, the CuI -$Fe_3O_4@SiO_2$ *(EDTA)* catalyst was prepared through a straightforward and green procedure (Scheme 1).

2.3 | Mushroom tyrosinase inhibition assay

Diphenolase activity of mushroom tyrosinase was determined using L-DOPA as the substrate, and by observing the formation of dopachrome at 475 nm as reported in our previous studies.[23,24,77–79] Initially, stock solutions of test compounds in DMSO at 40 mM were prepared and diluted to the required concentrations. Then after 10 ml of tyrosinase (0.5 mg/ml) was mixed with 160 ml of phosphate buffer (50 mM, pH = 6.8) in 96-well plates and 10 ml of the test compounds at different concentrations were added to each well (in triplicate). The plates were incubated at 28 °C for 20 min, then 20 ml of L-DOPA solution (0.5 mM) was added to the wells. Kojic acid was used as a positive control, and the experiments were done in three independent runs. The inhibitory activity of the tested samples was stated in terms of IC_{50}, which is the concentration that inhibited 50% of the enzyme activity. The percent inhibition ratio was assessed according to the following equation:

$$\text{Inhibition}\,(\%) = 100\left(\text{Abs}_{\text{control}} - \text{Abs}_{\text{compound}}\right)/\text{Abs}_{\text{control}}$$

3 | RESULTS AND DISCUSSION

3.1 | Design strategy

Molecular hybridization is a powerful tool in drug design and development that is based on the combination of pharmacophoric fragments of biologically active molecules. The target 5-((1-benzyl-1,2,3-triazol-4-yl)methoxybenzylidene)-2-(arylamino)thiazol-4-one skeleton was designed based on the structures of some tyrosinase inhibitors stated in our previous studies and other literature (Figure 1). Some thiazolidine-2,4-dione derivatives (**A** in

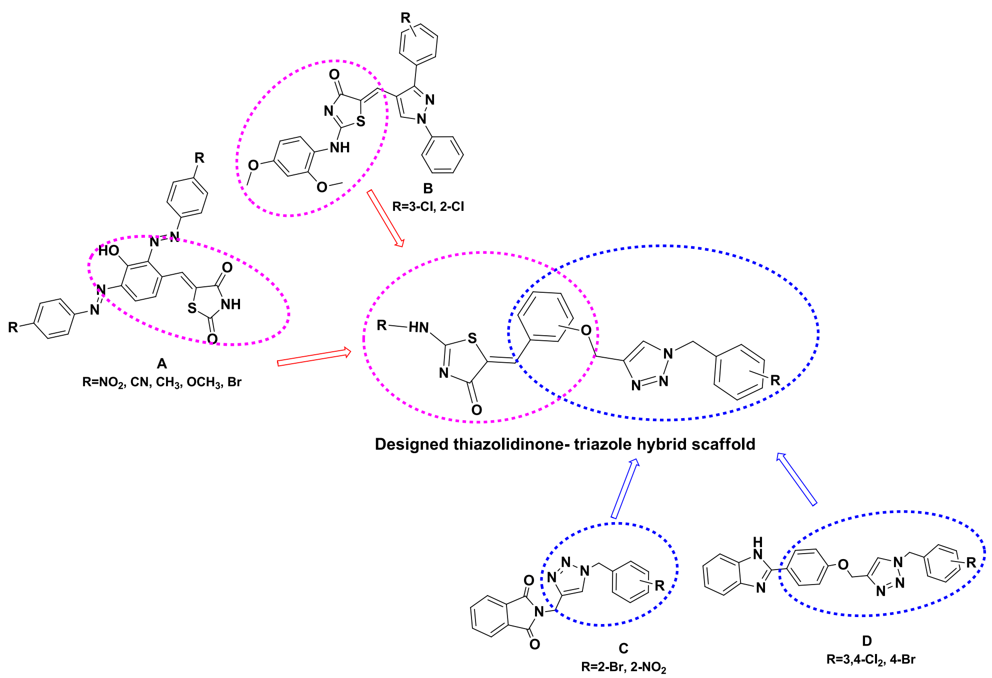

FIGURE 1 Design of proposed thiazolone-triazole hybrids as tyrosinase inhibitors using molecular hybridization approach

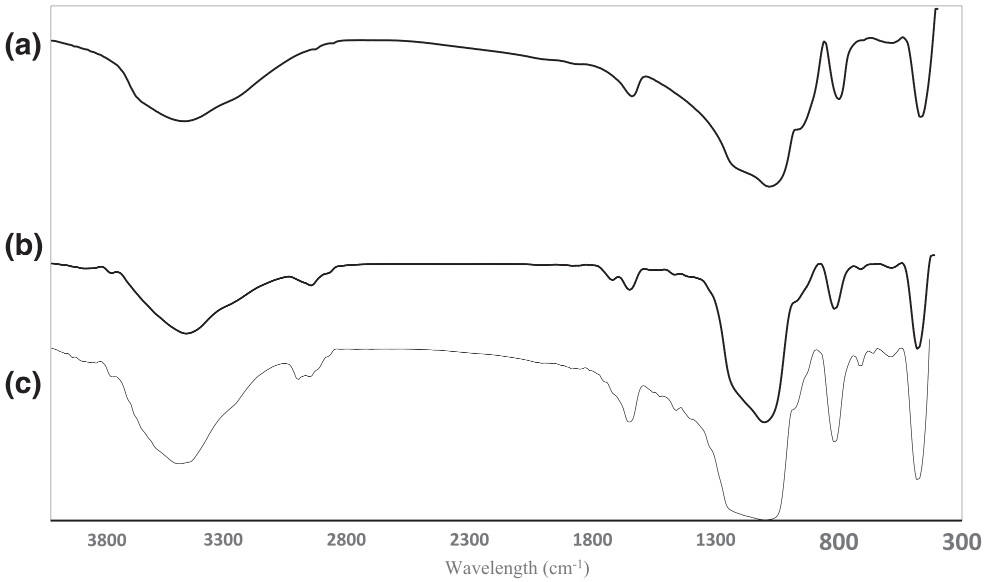

FIGURE 2 FT- IR spectra of (a) Fe_3O_4@SiO_2 MNPs, (b) Fe_3O_4@SiO_2 *(TMS-EDTA)* and (c) CuI supported-Fe_3O_4 @ SiO_2*(TMS-EDTA)*

Figure 1) have been reported to exhibit tyrosinase inhibitory activity (IC_{50}s = 37.6–140.3 μM).[26] Furthermore, it has been found that two 2-(2,4-dimethoxy phenylamino)-5 methylene-4-thiazolinone derivatives (**B** in Figure 1) with IC_{50} values of 34.1 and 52.6 μM were effective tyrosinase inhibitors.[25] Our previous study indicated that two phthalimide-1,2,3-trizole hybrid compounds (**C** in Figure 1) showed less inhibitory activity on tyrosinase ((IC_{50}s = 26.2 and 26.5 μM) than the reference drug kojic acid did.[24] Moreover, it was proved that benzimidazole-1,2,3-triazole hybrid compounds (**D** in Figure 1) exhibited effective inhibitory activity comparable to that of kojic acid with IC_{50} values of 9.42 and 10.34 μM which were comparable to that of kojic acid (IC_{50} = 9.28 μM).[23] Considering these structural features, we designed a series of thiazolone-triazole hybrids as tyroinase inhibitors by applying hybridization approach.

3.2 | Characterization of copper iodide Fe_3O_4@SiO_2 (TMS-EDTA)

The CuI supported-Fe_3O_4@SiO_2 *(TMS-EDTA)* nanoparticle was synthesized for the first time and also characterized by FTIR, TGA, TEM, BET, BJH, XRD, EDAX and FESEM analysis. In Figure 2, the IR spectra of

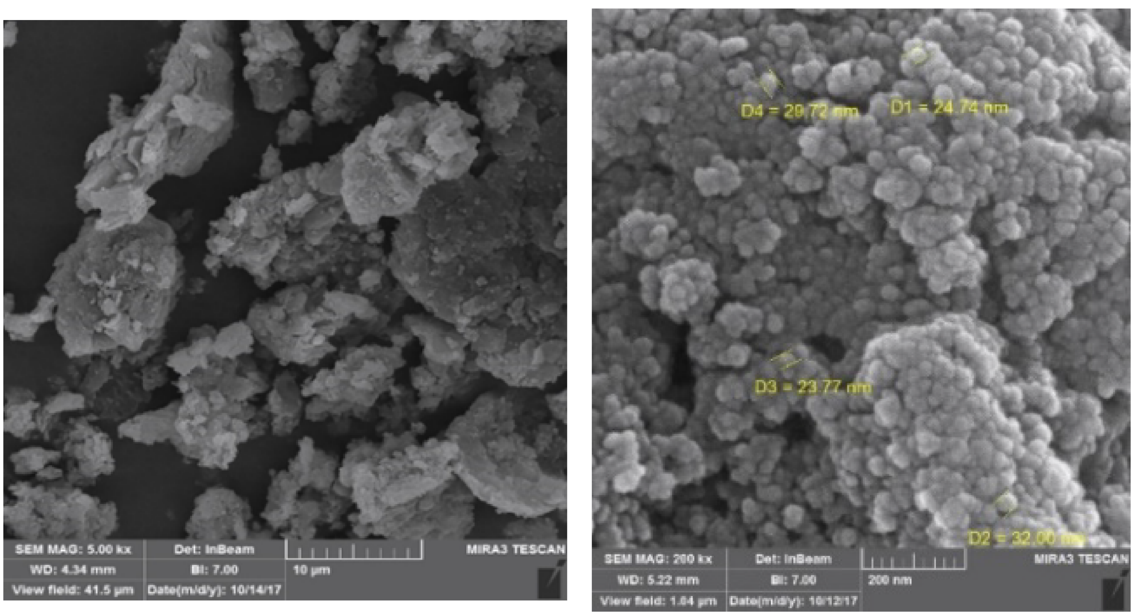

(a) (b)

FIGURE 3 FESEM images of CuI/Fe_3O_4@SiO_2(TMS-EDTA) nanoparticles

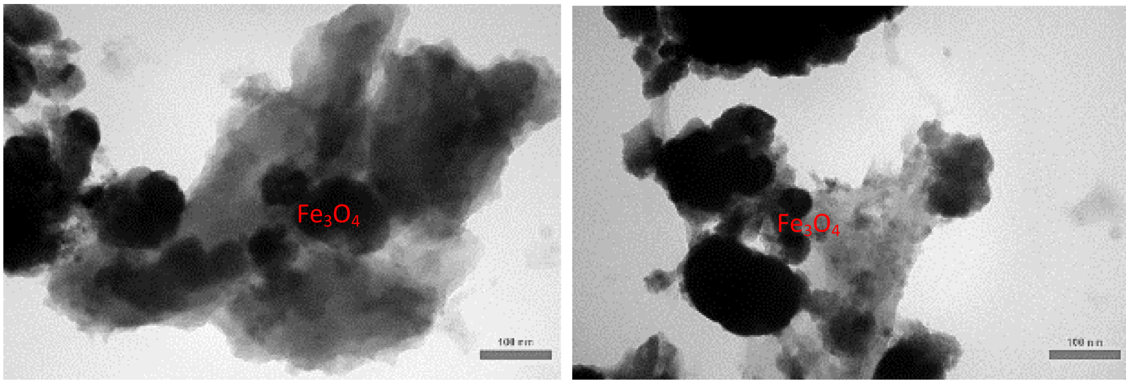

(a) (b)

FIGURE 4 TEM images of (a) Fe_3O_4 @ SiO2(TMS-EDTA) nanoparticles and (b) CuI/Fe_3O_4@SiO_2(TMS-EDTA) nanoparticles

Fe_3O_4@SiO_2 magnetic nanoparticle (a), Fe_3O_4@SiO_2 (*TMS-EDTA)* (b) and CuI/-Fe_3O_4@SiO_2 (*TMS-EDTA)* (c) were demonstrated. As illustrated in the IR spectrum of Fe_3O_4@SiO_2 MNP in Figure 2(a), the characteristic peaks at 551 cm^{-1} and 572 cm^{-1} is related to Fe–O, which confirms the existence of Fe_3O_4. The FT-IR data for Fe_3O_4@SiO_2 (*TMS-EDTA)* (Figure 2b) displays two peaks at 1660, and 1,385 $cm^{-1,}$ which attributed to C=O and C-N groups of ligand, respectively and stretching vibration of Si–O at 1050, 1110 cm^{-1} are assignable for the Fe_3O_4@SiO_2 (*TMS-EDTA).* The FT-IR data for copper complex-Fe_3O_4@SiO_2 (*TMS-EDTA)* (Figure 2c) is the appearance of a peak at 806.61 cm^{-1} for Cu–O stretching vibration.[72]

In order to prove some properties as the average particle size and morphology of catalyst structure, the field emission scanning electron microscopy (FESEM) images were used where clearly shows copper iodide homogeneously immobilized on the Fe_3O_4@SiO_2 (*TMS-EDTA)* surface (Figure 3). Furthermore, the aggregation of this copper modified-nanoparticles was investigated by the transmission electron microscopy (TEM) analysis. The TEM images (Figure 4) of MNPs showed a well-defined morphology of particles and confirmed nano-sized particles distributing in the catalyst matrix, which had a diameter around 20–40 nm. The MNPs aggregation is due to the preparation of the TEM sample throughout the solvent evaporation the NPs aggregate on the grid.[75,76]

The X-ray diffraction (XRD) pattern shows characteristic peaks of copper, presenting all the phases of Cu, as shown in Figure 5 (b). The XRD was investigated with Philips PW1730 diffractometer with CuKα radiation (λ = 1.5418 Å) within a range of Bragg angle 10-80 at 40 kV indicating the presence of nanoparticles such as Fe_3O_4, SiO_2, and Cu into the catalyst. As displayed, the XRD pattern of CuI supported-Fe_3O_4@SiO_2(TMS-EDTA) nanoparticle indicates some characteristic peaks at 2θ values:74, 62, 56, 52, 43, 35, 30, and 25 corresponding diffractions are in good agreement with those results for Fe_3O_4 @ SiO_2.[72] The diffraction peak shows a slight

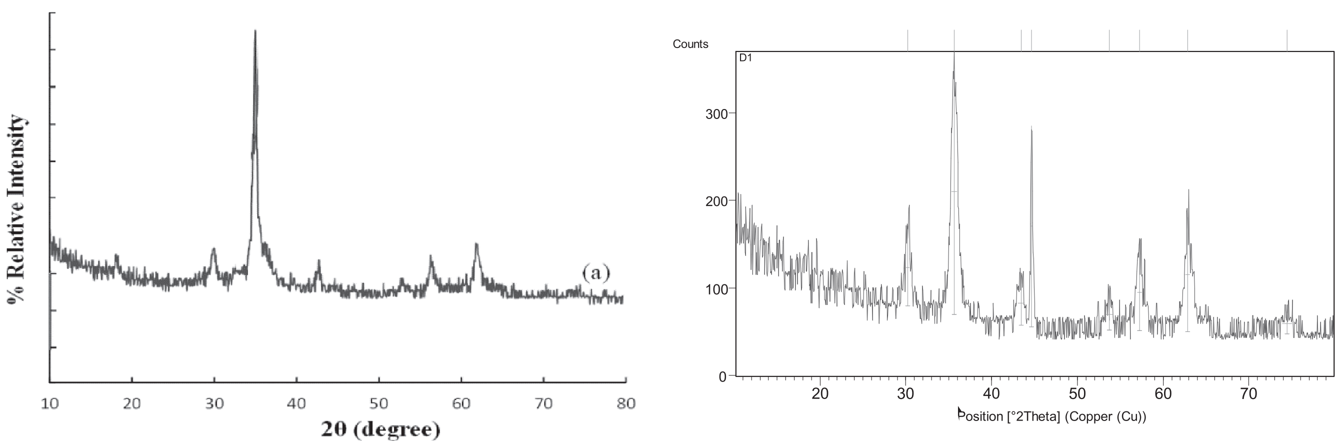

(a) (b)

FIGURE 5 XRD pattern of (a) Fe_3O_4@SiO_2 and (b) CuI/-Fe_3O_4@SiO_2 (*TMS-EDTA)*

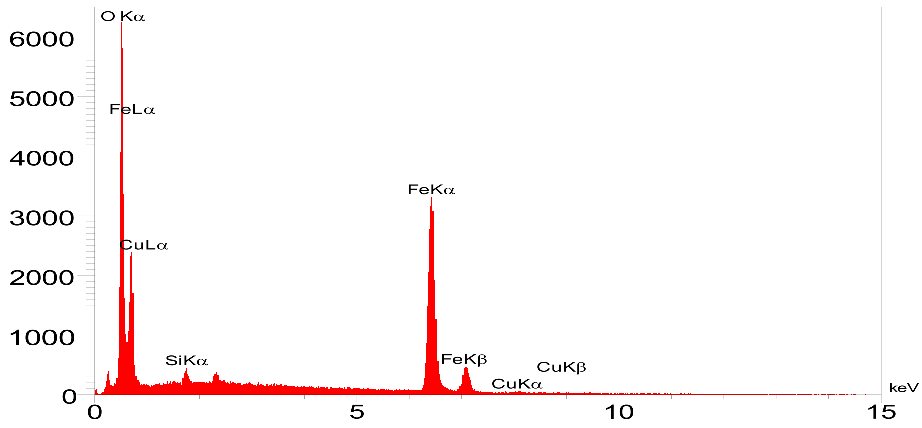

Elt	Line	Int	Error	K	Kr	W%	A%
O	Ka	706.3	53.4750	0.3651	0.2967	40.76	69.73
Si	Ka	23.9	0.3423	0.0137	0.0112	1.65	1.58
Fe	Ka	817.0	5.4789	0.5987	0.4924	55.34	26.59
Cu	Ka	3.1	0.2350	0.0225	0.0220	2.25	2.10
				1.0000	0.8223	100.00	100.00

FIGURE 6 EDAX of CuI/Fe_3O_4@ SiO_2(*TMS-EDTA*) nanoparticle

decline intensity along with peak expansion, which may be attributed to decreasing of scattering contrast arises from Fe_3O_4@SiO_2 surface and the organic moiety immobilized onto it (Figure 5 (a) and (b)).

The particles size was calculated by Scherrer equation (1)

$$\mathrm{L = K\lambda/(B\cos\theta)}L = \frac{K\lambda}{B\cos\theta}L = \frac{K\lambda}{B\cos\theta}L = \frac{K\lambda}{B\cos\theta}L = \frac{K\lambda}{B\cos\theta} \tag{1}$$

where the broadening radian is defined λ, obtaining from the full width at half maximum, θ is the Bragg angle, and k is the Scherrer constant (0.9 for Cu Kα radiation). The calculated particle size through this equation is about 17.7 nm.

These results are supported by SEM data. Energy dispersive spectroscopy analysis of X-rays (EDAX) data for the CuI supported-Fe_3O_4@SiO_2 (*TMS-EDTA*)

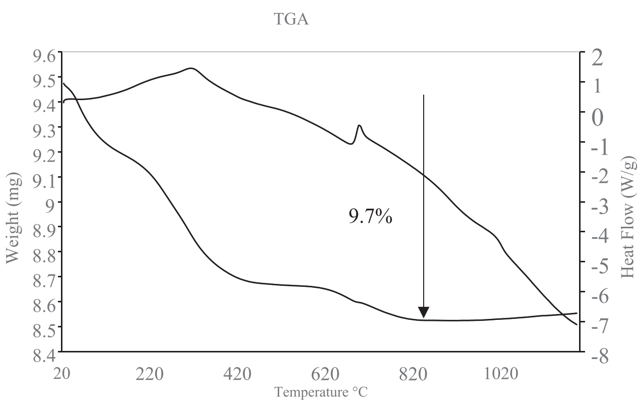

FIGURE 7 TGA copper supported of Fe_3O_4@ SiO_2(TMS-EDTA) nanoparticle

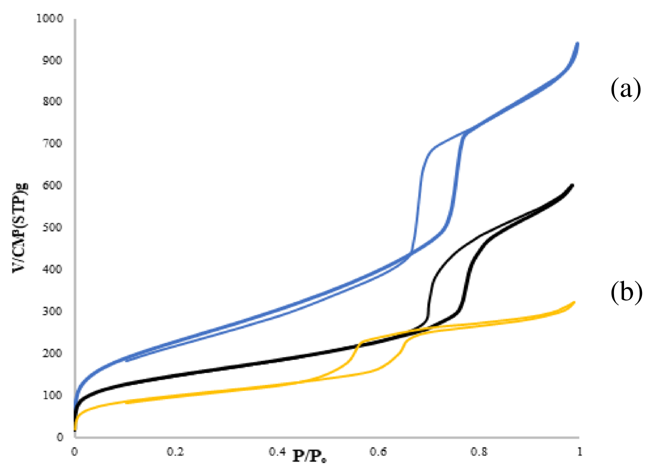

FIGURE 8 N2 adsorption–desorption isotherms of Fe_3O_4@SiO_2 MNPs, (b) Fe_3O_4@SiO_2 *(TMS-EDTA)* and (c) CuI supported-Fe_3O_4 @ SiO_2*(TMS-EDTA)*

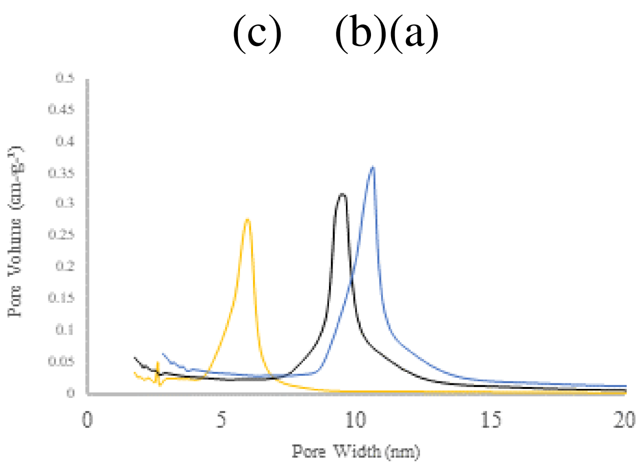

FIGURE 9 BJH pore size distribution curves of (a) $Fe_3O_4@SiO_2$ MNPs, (b) $Fe_3O_4@SiO_2$ *(TMS-EDTA)* and (c) CuI supported-Fe_3O_4 @ SiO_2*(TMS-EDTA)*

nanocatalyst was illustrated in Figure 6. The EDAX analysis confirms that the Cu is existing on the surface of the matrix. This analysis proved that the Cu characteristic peaks in 2.25% weight percentage. Also, The TGA curves of copper iodide supported-$Fe_3O_4@SiO_2$ *(TMS-EDTA)* shown in Figure 7.

The thermal stability of the synthesized NPs was examined by thermo-gravimetric analysis. The decomposition of copper iodide supported-$Fe_3O_4@SiO_2$ (TMS-EDTA) displays the first weight loss below 200 °C, and this can be considered to the desorption of physically adsorbed water in addition to dehydration of the surface –OH groups. The first stage of the endothermic weight loss could be related to the evaporation of water almost 170–210 °C (3.7%), that physically absorbed on the surface of the nanoparticle. The second stage of the weight loss could be allocated to the decomposition of O-containing functional groups. Eventually, the major weight loss occurs above 300 °C, corresponding to the degradation of carbon skeletons within apparent mass change (9.7%). Also, Fe_3O_4 changed to Fe_2O_3 in temperature higher than 700 °C. Moreover, relatively slow weight loss at elevated temperatures can be related to the disintegration of the silica. So, the TGA curves confirm the successful grafting of organic groups onto the MNP.

The nitrogen adsorption–desorption isotherms and the BJH pore size distribution (based on the adsorption branch of the isotherms) for all samples $Fe_3O_4@SiO_2$ MNPs, $Fe_3O_4@SiO_2$ *(TMS-EDTA)* and CuI supported-Fe_3O_4 @ SiO_2*(TMS-EDTA)* are shown in Figure 8 and Figure 9. Type IV characterizes the isotherms with an H1-type hysteresis loop well-defined by IUPAC, representing that the well-ordered arrangement of $Fe_3O_4@SiO_2$ has stayed. Table 1 presents the results for three structural parameters of the samples, including specific surface area (BET method), total pore volume, and pore diameter (BJH method). Successful incorporation of functional organic materials into $Fe_3O_4@SiO_2$ *(TMS-EDTA)* pores and the inclusion of Cu into this

TABLE 1 N_2 adsorption–desorption isotherms of (a)$Fe_3O_4@SiO_2$ MNPs, (b) $Fe_3O_4@SiO_2$ (TMS-EDTA) and (c) CuI supported-Fe_3O_4 @ SiO_2(TMS-EDTA)

Material Type	Surface Area (m^2g^{-1})	Pore Volume (cm^3g^{-1})	Pore size (nm)
$Fe_3O_4@SiO_2$	898	0.99	9.922
$Fe_3O_4@SiO_2$ (TMS-EDTA)	789	0.862	8.211
CuI-Fe_3O_4 @ SiO_2(TMS-EDTA).	351.7	0.498	5.206

SCHEME 2 Preparation of starting materials

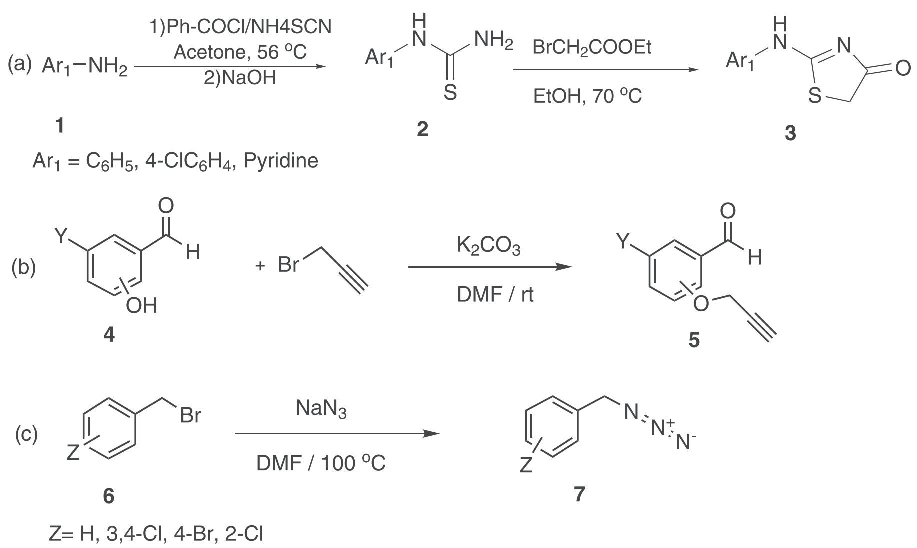

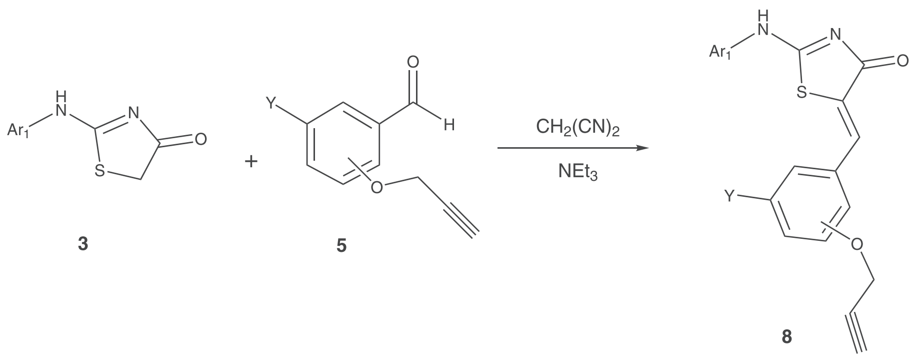

SCHEME 3 Preparation of the 2-arylamino-5-(propynyloxy) benzylidene) 4-thiazolidinone derivatives

structure shifted the pore size to a smaller value and led to declining in pore volume and surface area.

Based on the obtained experimental results, it can be predicted that the copper supported-Fe_3O_4@SiO_2 (TMS-EDTA) could be used as a heterogeneous nanocatalyst with high catalytic activity in the 1,2,3-triazoles synthesis. Therefore, the efficiency of copper iodide supported-Fe_3O_4@SiO_2 (*TMS-EDTA)* nanocatalyst was tested in the thiazolone-triazole cycloadducts synthesis through a straightforward and green procedure.

3.3 | Thiazolone-1,2,3-triazole analogs

As shown in Scheme 2, initially, 5-arylidene-4-thiazolone derivatives **3a-c** were synthesized as the tautomeric mixtures in accordance with the literature (Scheme 2a).[80,81] In the following, compounds **5a-c** were prepared from hydroxy benzaldehyde **4a-c** and propargyl bromide in the presence of K_2CO_3 by a known method (Scheme 2b).[82] The general procedure for the preparation of organic azides is shown in Scheme 2c.[83]

Then, dipolarophiles **8a-c** were synthesized by the reaction of thiazolone derivatives **3a-c** with propargylated hydroxyl benzaldehydes **5a-c** in the presence of malononitrile as a catalyst under reflux condition in good yields. The active methylene in the thiazolones **3a** goes through nucleophilic addition reaction to the double bond of arylidene malononitriles *via* a Michael type addition reaction to give dipolarophile **8a** (Scheme 3).

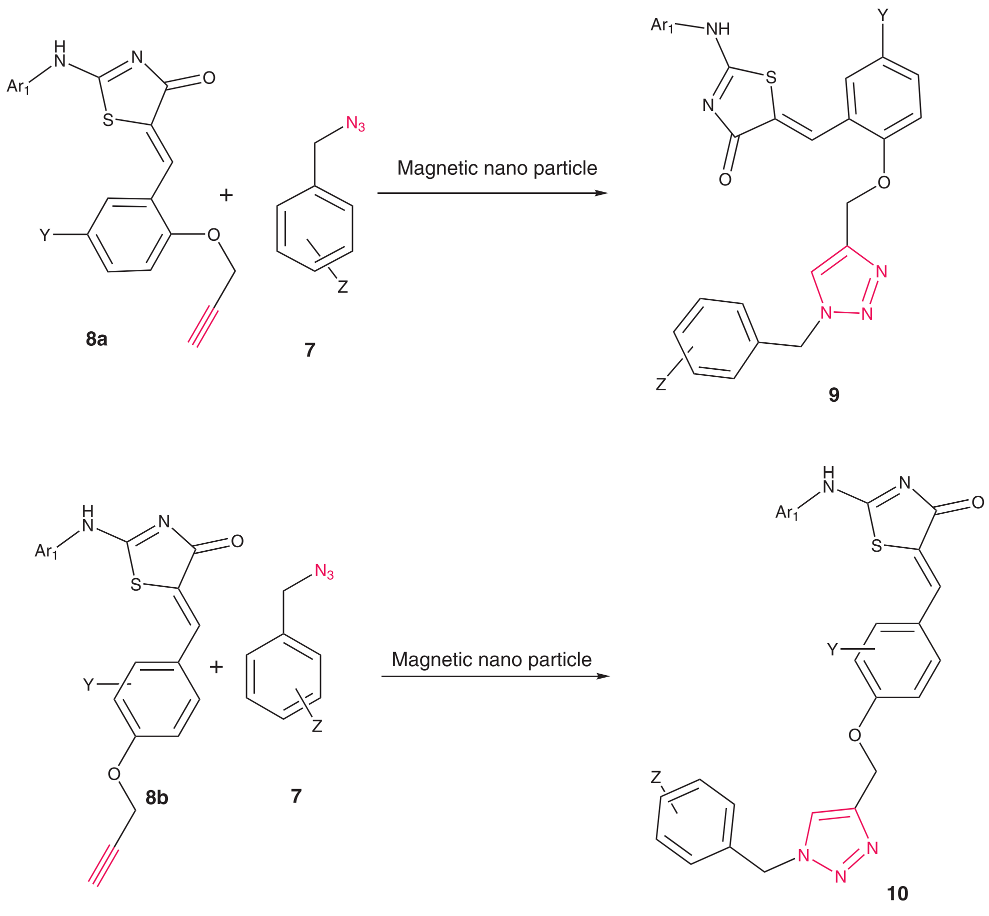

SCHEME 4 CuAAC reaction between alkyne and benzyl azide

TABLE 2 Optimization of cycloaddition to generate **9a**

Entry	Catalyst	Solvent	Catalyst (mol%)	Yield, %
1	$CuSO_4$	DMSO	5	80
2	$CuSO_4$	DMSO-Water	5	90
3	$CuSO_4$	Water	5	65
4	CuI-Fe_3O_4@SiO_2 (TMS-EDTA)	Water	5	78
5	CuI-Fe_3O_4@SiO_2 (TMS-EDTA)	Ethanol	10	78
6	CuI-Fe_3O_4@SiO_2 (TMS-EDTA)	Ethanol	5	**97**
7	CuI-Fe_3O_4@SiO_2 (TMS-EDTA)	Ethanol	10	93

As exhibited in Scheme 4, under the optimized conditions, different substituted alkyne **8** and benzyl azide **7** were used in this 32CA reaction (Table 2), and an array of novel thiazolone triazoles was synthesized smoothly in good yields in the presence of CuI/Fe_3O_4@SiO_2(TMS-EDTA) nanoparticles and sodium ascorbate. The catalytically active Cu(I) species which supported on the functionalized Fe_3O_4@SiO_2(TMS-EDTA) nanoparticles can be generated from Cu (II) salts using sodium ascorbate as the reducing agent. These results are presented in Table 3.

In the presented work, due to biological properties of novel synthesized thiazolone incorporated triazole scaffold and high yield of the reaction, the pure product can be obtained through the addition of prepared magnetic nanoparticle and also the catalyst separated by an external magnet which there is no need to use of toxic solvent.

The products of cycloaddition reaction exist as a mixture of tautomeric cycloadduct **9a** and **9a'** in ethanol solution (Figure 10). The structure of the cycloadduct **9** was assigned by various spectroscopic techniques. So, the IR spectrum of yellow solid **9a** demonstrated absorptions at 3354 cm^{-1}, indicating the presence of an NH group, 1,686 cm^{-1} of a CO group, 1,540 for imine

TABLE 3 Copper-catalyzed 1,3 dipolar cycloaddition of alkynes and azides

Entry	Ar	Y	Z	Yield
9a	Ph	H	H	97%
9b	Ph	H	3,4-Cl	75%
9c	Ph	H	4-Br	71%
9d	Py	H	4-Br	82%
9e	Py	H	2-Cl	81%
9f	Py	5-Br	H	85%
9 g	Py	H	3,4-Cl	86%
9 h	4-ClC_6H_4	H	2-Cl	58%
10a	Ph	H	H	83%
10b	Ph	H	3,4-Cl	79%
10c	Ph	3-OMe	H	77%
10d	Ph	3-OMe	2-Cl	70%
10e	Ph	3-OMe	3,4-Cl	73%
10f	Py	3-OMe	2-Cl	72%
10 g	Py	H	3,4-Cl	78%
10 h	Py	3-OMe	3,4-Cl	80%
10i	4-ClC_6H_4	H	H	63%
10j	4-ClC_6H_4	3-OMe	2-Cl	65%
10 k	4-ClC_6H_4	3-OMe	H	69%
10 l	4-ClC_6H_4	H	2-Cl	73%
10 m	4-ClC_6H_4	3-OMe	3,4-Cl	75%

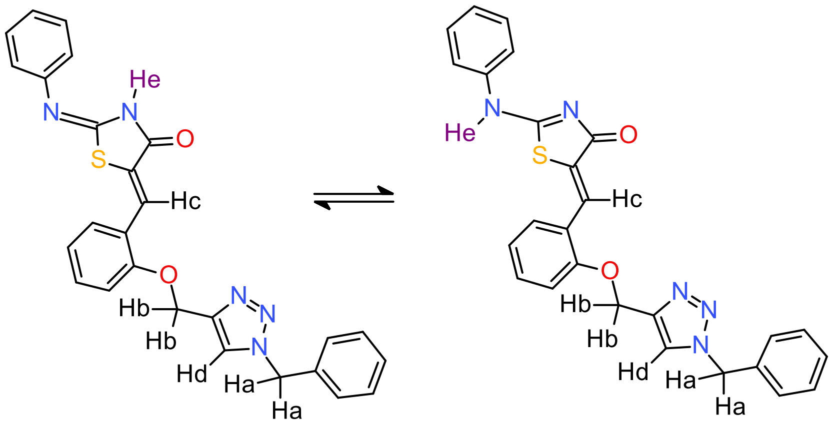

FIGURE 10 Two regioisomers of **9a**

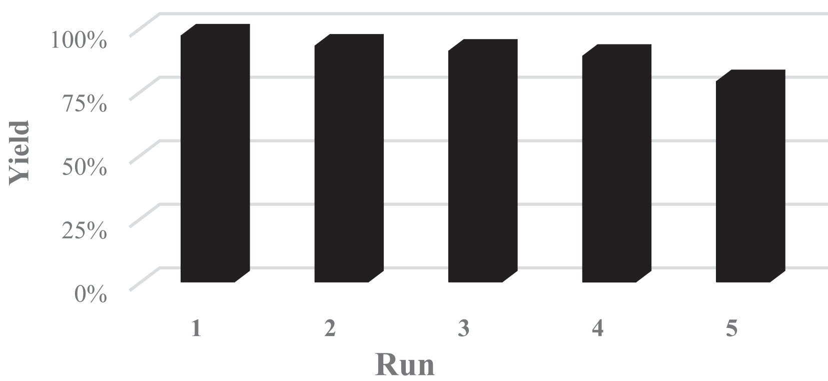

FIGURE 11 Recyclability of the Cu-Fe_3O_4@ SiO_2(TMS-EDTA) nanoparticle in the click reactions

group and at 1176 cm^{-1} which corresponds to ether group. The ^1H NMR spectrum of **9a** exhibited a singlet at $\delta = 7.90$ for H_d, two singlet peaks of -CH_2 groups at 5.26 and 5.30 ppm for H_a in **9a**, and a singlet peak at 5.63 ppm for H_b in OCH_2 group, respectively. Two singlet peaks at 8.30 ppm and 8.34 ppm of CH is referred to H_c of methine group. Two signals at 11.54 and 12.34 of NH represent the existence of a tautomeric mixture of **9a**. The ^{13}C NMR of **9** showed a peak at $\delta = 53.32$ ppm owing to the CH_2 group and a peak at $\delta = 62.13$ ppm for the CH_2 attached to the oxygen group. The NMR spectral data of isolated product was in good agreement with the assigned structure of **9a** and **9a'**. Mass spectra also confirmed the formation of the product. The mass spectrum of **9a** showed a molecular ion peak of 467.1 (M^+). This procedure was applied to a series of organic azides

TABLE 4 Assessment of the catalyst activity in comparison with previous work

Entry	Substrate of Benzyl	Catalyst	Conditions	Time (min)	Yield (%)
1	Benzyl bromide	Polymer supported CuI and azide	Reflux, Ethanol	60	92[84]
2	Benzyl bromide	$CuCl_2/SiO_2$	H_2O, MW/70 °C	10	92[85]
3	Benzyl bromide	Cu/Al_2O_3	Ball-mill	60	92[86]
4	Benzyl bromide	CuNPs	Methanol, r.t.	480	93[87]
5	Benzyl bromide	CuNPs/C	H_2O, 70 °C	180	98[87]
6	Benzyl bromide	Cu(I)-zeolite	H_2O, 90 °C	15	90[88]
7	Benzyl azide	$CuSO_4$-Chitosan	H2O, r.t.	240	99[89]
8	Benzyl azide	$MnFe_2O_4$@GO@CS/Cu	H_2O/EtOH, 50 °C	30	95[90]
9	Benzyl azide	$CuSO_4$	DMSO	180	80 [this work]
10	Benzyl azide	$CuSO_4$	DMSO-Water	220	90, [this work]
11	Benzyl azide	$CuSO_4$	Water	150	65, [this work]
12	Benzyl azide	CuI-Fe_3O_4@SiO_2 (TMS-EDTA)	Ethanol	120	**97, [**this work]

and terminal alkynes under similar conditions to form the corresponding triazole products in good yields (Supporting information-Spectra: Fig 1-48, spectral interpretation **3a-10m**).

3.4 | Comparison of the catalyst

The result for CuI-Fe_3O_4@SiO_2 (TMS-EDTA) catalyst performance evaluation as well as the activity information of the previously reported heterogeneous copper particles are presented in Table 4. Consequently, the synthesized catalyst has some beneficials, such as stability, slightly less reaction time at room temperature, separable magnetically, and the available commercial materials at a suitable price.

3.5 | Recycling of the catalyst

The heterogeneous catalysts recyclability is essential from the economic perspective. The method of reusing the CuI-Fe_3O_4@SiO_2 (TMS-EDTA) catalyst was manipulated for the click reaction of organic azides and terminal alkynes upon optimized reaction conditions. After the accomplishment of each cycle, the solid catalyst was separated from the reaction mixture using an external magnet and washed several times with ethanol (5 ml), and after drying through vacuum overnight and use again in a sequential run. The results in Figure 11 determine that the supported catalyst was highly recyclable under the studied reaction conditions, preserving almost unaltered its initial catalytic performance after six uses.

3.6 | Anti-tyrosinase activity of the synthesized thiazolone -triazoles

The mushroom tyrosinase inhibitory potency of some derivatives was assessed using kojic acid as the common inhibitor. Results in terms of IC_{50} values are presented in Table 5. Compounds **9a** , **9c** , **9e** and **9 g** with IC_{50} values of 8.92 ± 1.95, 9.81 ± 2.20, 6.34 ± 0.87, 5.90 ± 1.23 μM, respectively, were found to be considerably better tyrosinase inhibitors than the positive control kojic acid (IC_{50} = 18.36 ± 1.09 μM). Compounds **9b** and **10b** exhibited tyrosinase inhibition with IC_{50} values of 47.23 ± 2.80 and 49.4 ± 1.78 μM, respectively.

According to IC_{50} values in Table 5, it can be affirmed that group **9** derivatives possessing 2-((1-aryl-1,2,3-triazole-4-yl) methoxy) benzylidene moieties, were considerably more potent tyrosinase inhibitors than their counterparts in group **10** bearing 4-((1-aryl-1,2,3-triazole-4-yl)methoxy)benzylidene moieties (comparing **9a**, **9b** and **9 g**, respectively, with **10a**, **10b** and **10 g**). Moreover, in group 9 compounds, the presence of a pyridine ring substitution at the amino-phenyl group, as in **9 g**, would remarkably improve the activity as compared to **9b**.

TABLE 5 Tyrosinase inhibitory activities of synthesized compounds **9a-9 h**, **10a-10 m** and kojic acid

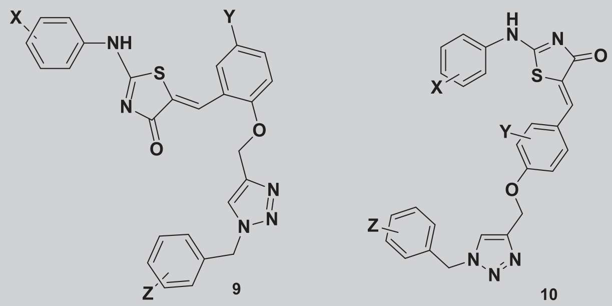

Compounds	X	Y	Z	IC_{50} (μM)[a]
9a	H	H	H	8.92 ± 1.65
9b	H	H	3,4-Cl	47.23 ± 2.80
9c	H	H	4-Br	9.81 ± 2.20
9d	Py	H	4-Br	ND[b]
9e	Py	H	2-Cl	6.34 ± 0.87
9f	Py	5-Br	H	>50
9 g	Py	H	3,4-Cl	5.90 ± 1.23
9 h	4-Cl	H	2-Cl	ND
10a	H	H	H	>50
10b	H	H	3,4-Cl	49.4 ± 1.78
10c	H	3-OMe	H	ND
10d	H	3-OMe	2-Cl	>50
10e	H	3-OMe	3,4-Cl	ND
10f	Py	3-OMe	2-Cl	ND
10 g	Py	H	3,4-Cl	>50
10 h	Py	3-OMe	3,4-Cl	ND
10i	4-Cl	H	H	ND
10j	4-Cl	3-OMe	2-Cl	ND
10 k	4-Cl	3-OMe	H	ND
10 l	4-Cl	H	2-Cl	ND
10 m	4-Cl	3-OMe	3,4-Cl	ND
Kojic Acid	H	H	H	18.36 ± 1.09

[a]Values represent means ± SE of 3 independent experiments.
[b]ND; Not determined.

4 | CONCLUSION

In summary, we prepared a new copper supported core-shell magnetic nanoparticle catalyst and examined its efficiency in the synthesis of novel thiazolone −1,4-triazole analogues through 32CA reaction of azides and substituted alkynes. This magnetic nanoparticle was applied to the click reactions to give some new triazole scaffolds under green and mild conditions in high yields (60–97%) and moderately short reaction time. In these reactions, a low amount of catalyst is required, which is recoverable through a simple filtration process and can be reused for five runs with no considerable catalytic activity loss. The performance of our catalyst was investigated to develop a facile preparation protocol having advantages including low cost, easily available materials, reduce reaction time, easy workup, and environmental friendliness. Some of the synthesized derivatives were tested for their mushroom tyrosinase inhibitory activity. Compounds **9a**, **9c**, **9e**, and **9 g** showed promising antityrosinase activity with IC_{50} values considerably lower than the reference inhibitor kojic acid.

ACKNOWLEDGMENTS

We gratefully acknowledge the financial support from the Research Council of University of Mazandaran.

AUTHOR CONTRIBUTIONS

Mahdieh Darroudi: Conceptualization; data curation; formal analysis; investigation; project administration. **Sara Ranjbar:** Formal analysis. **Mohammad Esfandiar:** Methodology. **Mahsima Khoshneviszadeh:** Investigation; resources. **Mahshid Hamzehloueian:** Supervision; validation. **Mehdi khoshneviszadeh:** Project administration; resources; supervision. **Yaghoub Sarrafi:** Funding acquisition; resources; supervision.

ORCID

Mahdieh Darroudi https://orcid.org/0000-0002-9152-2642
Sara Ranjbar https://orcid.org/0000-0002-7675-4146
Mohammad Esfandiar https://orcid.org/0000-0003-2801-1142
Mahsima Khoshneviszadeh https://orcid.org/0000-0002-6993-4624
Mahshid Hamzehloueian https://orcid.org/0000-0001-8388-9260
Mehdi Khoshneviszadeh https://orcid.org/0000-0003-1458-2964
Yaghoub Sarrafi https://orcid.org/0000-0002-1351-9720

REFERENCES

[1] R. Alvarez, S. Velazquez, A. San-Felix, S. Aquaro, E. De Clercq, C.-F. Perno, A. Karlsson, J. Balzarini, M. J. Camarasa, *J. Med. Chem.* **1994**, *37*, 4185.
[2] F. D. da Silva, M. C. de Souza, I. I. Frugulhetti, H. C. Castro, L. D. Silmara, T. M. de Souza, D. Q. Rodrigues, A. M. Souza, P. A. Abreu, F. Passamani, C. R. Rodrigues, *Eur. J. Med. Chem.* **2009**, *44*, 373.
[3] D. R. Buckle, C. J. Rockell, H. Smith, B. A. Spicer, *J. Med. Chem.* **1986**, *29*, 2262.
[4] J. C. Fung-Tomc, E. Huczko, B. Minassian, D. P. Bonner, *Antimicrob. Agents Chemother.* **1998**, *42*, 313.
[5] H. T. Fahmy, *Boll. Chim. Farm.* **2000**, *140*, 422.
[6] N. Karali, E. İllhan, A. Gürsoy, M. Kiraz, *Farm.* **1998**, *53*, 346.
[7] N. Cesur, Z. Cesur, N. Ergenc, M. Uzun, *Arch. Pharm.* **1994**, *327*, 271.
[8] R. Périon, V. Ferrières, M. Isabel García-Moreno, C. Ortiz Mellet, R. Duval, J. M. García Fernández, D. Plusquellec, *Tetrahedron* **2005**, *61*, 9118.
[9] D. J. Anderson, M. R. Barbachyn, D. E. Emmert, S. A. Garmon, D. R. Graber, *J. Med. Chem.* **2000**, *43*, 953.
[10] S. A. Bakunov, S. M. Bakunova, T. Wenzler, M. Ghebru, K. A. Werbovetz, R. Brun, R. R. Tidwell, *J. Med. Chem.* **2010**, *53*, 254.
[11] A. Rao, A. Carbone, A. Chimirri, E. De Clercq, A. M. Monforte, P. Monforte, C. Pannecouque, M. Zappalà, *Farm.* **2002**, *57*, 747.
[12] M. L. Barreca, A. Chimirri, L. De Luca, A. M. Monforte, P. Monforte, A. Rao, M. Zappal, J. Balzarini, E. De Clercq, C. Pannecouque, M. Witvrouw, *Bioorg. Med. Chem. Lett.* **2001**, *11*, 1793.
[13] A. Rao, J. Balzarini, A. Carbone, A. Chimirri, E. De Clercq, A. M. Monforte, P. Monforte, C. Pannecouque, M. Zappalà, *Farmaco* **2004**, *59*, 33.
[14] M. Hoshino, *Nature* **1960**, *186*, 174.
[15] A. M. Thompson, A. Blaser, R. F. Anderson, S. S. Shinde, S. G. Franzblau, Z. Ma, W. A. Denny, B. D. Palmer, *J. Med. Chem.* **2009**, *52*, 637.
[16] A. K. Jordão, V. F. Ferreira, E. S. Lima, M. C. B. V. de Souza, E. C. L. Carlos, *Bioorg. Med. Chem.* **2009**, *17*, 3713.
[17] D.-R. Hou, S. Alam, T.-C. Kuan, M. Ramanathan, T.-P. Lin, M.-S. Hung, *Bioorg. Med. Chem. Lett.* **2009**, *19*, 1022.
[18] J. Shen, R. Woodward, J. P. Kedenburg, X. Liu, M. Chen, L. Fang, D. Sun, P. G. Wang, *J. Med. Chem.* **2008**, *51*, 7417.
[19] C. G. Bonde, N. J. Gaikwad, *Bioorg. Med. Chem.* **2004**, *12*, 2151.
[20] S. G. Kucukguzel, E. E. Oruc, S. Rollas, F. Sahin, A. Ozbek, *Eur. J. Med. Chem.* **2002**, *37*, 197.
[21] Ö. Ateş, H. Altintaş, G. Ötük, *Arzneimittelforschung* **2000**, *50*, 569.
[22] O. Ateş, A. Kocabalkanli, G. Saniş, A. Ekinci, *Arzneimittelforschung* **1997**, *47*, 1134.
[23] H. Rouh, Y. Liu, N. Katakam, L. Pham, Y. L. Zhu, G. Li, *J. Org. Chem.* **2018**, *83*, 15372.
[24] G. Wu, Y. Liu, Z. Yang, N. Katakam, H. Rouh, S. Ahmed, D. Unruh, K. Surowiec, G. Li, *Research* **2019**, *2019*, 1.
[25] Y. Liu, S. Ahmed, X. Y. Qin, H. Rouh, G. Wu, G. Li, B. Jiang, *Chem. - an Asian J.* **2020**, *15*, 1125.

[26] Y. Liu, G. Wu, Z. Yang, H. Rouh, N. Katakam, S. Ahmed, D. Unruh, Z. Cui, H. Lischka, G. Li, *Sci. China Chem.* **2020**, *63*, 692.
[27] M. Mahdavi, A. Ashtari, M. M. Khoshneviszadeh, S. Ranjbar, A. Dehghani, T. Akbarzadeh, B. Larijani, M. M. Khoshneviszadeh, M. Saeedi, *Chem. Biodiversity* **2018**, *15*, e1800120.
[28] M. B. Tehrani, P. Emani, Z. Rezaei, M. Khoshneviszadeh, M. Ebrahimi, N. Edraki, M. Mahdavi, B. Larijani, S. Ranjbar, A. Foroumadi, M. Khoshneviszadeh, *J. Mol. Struct.* **2019**, *1176*, 86.
[29] S. S. Gawande, S. C. Warangkar, B. P. Bandgar, C. N. Khobragade, *Bioorg. Med. Chem.* **2013**, *21*, 2772.
[30] M. Rezaei, H. T. Mohammadi, A. Mahdavi, M. Shourian, H. Ghafouri, *Int. J. Biol. Macromol.* **2018**, *108*, 205.
[31] S. Y. Seo, V. K. Sharma, N. Sharma, *J. Agric. Food Chem.* **2003**, *51*, 2837.
[32] S. Y. Lee, N. Baek, T. G. Nam, *J. Enzyme Inhib. Med. Chem.* **2016**, *31*, 1.
[33] T. Hasegawa, *Int. J. Mol. Sci.* **2010**, *11*, 1082.
[34] M. R. Loizzo, R. Tundis, F. Menichini, *Compr. Rev. Food Sci. Food Saf.* **2012**, *11*, 378.
[35] J. Hou, X. Liu, J. Shen, G. Zhao, P. G. Wang, *Expert Opin. Drug Discovery* **2012**, *7*, 489.
[36] A. Padwa, *1,3-Dipolar Cycloaddition Chemistry*, Wiley-Blackwell **1986**.
[37] C. W. Tornøe, C. Christensen, M. Meldal, *J. Org. Chem.* **2002**, *67*, 3057.
[38] S. Quader, S. E. Boyd, I. D. Jenkins, T. A. Houston, *J. Org. Chem.* **2007**, *72*, 1962.
[39] F. Himo, T. Lovell, R. Hilgraf, V. V. Rostovtsev, L. Noodleman, K. B. Sharpless, V. V. Fokin, *J. am. Chem. Soc.* **2005**, *127*, 210.
[40] Q. Wang, S. Chittaboina, H. N. Barnhill, *Lett. Org. Chem.* **2005**, *2*, 293.
[41] S. Díez-González, H. C. Kolb, M. G. Finn, K. B. Sharpless, *Catal. Sci. Technol.* **2011**, *1*, 166.
[42] J. E. Hein, V. V. Fokin, *Chem. Soc. Rev.* **2010**, *39*, 1302.
[43] V. D. Bock, H. Hiemstra, J. H. van Maarseveen, *European J. Org. Chem.* **2006**, *2006*, 51.
[44] Z. X. LIu, B. Bin Chen, M. L. Liu, H. Y. Zou, C. Z. Huang, *Green Chem.* **2017**, *46*, 6473.
[45] M. Darroudi, Y. Sarrafi, M. Hamzehloueian, *J. Serb. Chem. Soc.* **2018**, *83*, 821.
[46] F. Ilgen, B. König, *Green Chem.* **2009**, *11*, 848.
[47] A. K. Feldman, B. Colasson, V. V. Fokin, *Org. Lett.* **2004**, *6*, 3897.
[48] H. Sharghi, R. Khalifeh, M. M. Doroodmand, *Adv. Synth. Catal.* **2009**, *351*, 207.
[49] S. Kovács, K. Zih-Perényi, Á. Révész, Z. Novák, *Synthesis* **2012**, *44*, 3722.
[50] V. O. Rodionov, S. I. Presolski, S. Gardinier, Y. H. Lim, M. G. Finn, *J. am. Chem. Soc.* **2007**, *129*, 12696.
[51] P. Abdulkin, Y. Moglie, B. R. Knappett, D. A. Jefferson, M. Yus, F. Alonso, A. E. H. Wheatley, *Nanoscale* **2013**, *5*, 342.
[52] S. Lal, H. S. Rzepa, S. Díez-González, *ACS Catal.* **2014**, *4*, 2274.
[53] V. O. Rodionov, S. I. Presolski, D. D. Díaz, V. V. Fokin, M. G. Finn, *J. am. Chem. Soc.* **2007**, *129*, 12705.
[54] S. Azizi, N. Shadjou, M. Hasanzadeh, *Appl. Organomet. Chem.* **2020**, *34*. https://doi.org/10.1002/aoc.5321
[55] B. Kaboudin, Y. Abedi, T. Yokomatsu, *Org. Biomol. Chem.* **2012**, *10*, 4543.
[56] X. Q. Xiong, H. X. Chen, Z. K. Tang, Y. B. Jiang, *RSC Adv.* **2014**, *4*, 9830.
[57] H. Karimi-Maleh, O. A. Arotiba, *J. Colloid Interface Sci.* **2020**, *560*, 208.
[58] H. Karimi-Maleh, M. Shafieizadeh, M. A. Taher, F. Opoku, E. M. Kiarii, P. P. Govender, S. Ranjbari, M. Rezapour, Y. Orooji, *J. Mol. Liq.* **2020**, *298*, 112040.
[59] H. Karimi-Maleh, C. T. Fakude, N. Mabuba, G. M. Peleyeju, O. A. Arotiba, *J. Colloid Interface Sci.* **2019**, *554*, 603.
[60] F. Tahernejad-Javazmi, M. Shabani-Nooshabadi, H. Karimi-Maleh, *Compos. Part B Eng.* **2019**, *172*, 666.
[61] H. Karimi-Maleh, M. Sheikhshoaie, I. Sheikhshoaie, M. Ranjbar, J. Alizadeh, N. W. Maxakato, A. Abbaspourrad, *New J. Chem.* **2019**, *43*, 2362.
[62] R. Hao, R. Xing, Z. Xu, Y. Hou, S. Gao, S. Sun, *Adv. Mater.* **2010**, *22*, 2729.
[63] A.-H. Lu, E. L. Salabas, F. Schüth, *Angew. Chem., Int. Ed.* **2007**, *46*, 1222.
[64] R. N. Grass, E. K. Athanassiou, W. J. Stark, *Angew. Chem., Int. Ed.* **2007**, *46*, 4909.
[65] M. Gholinejad, N. Jeddi, *ACS Sustainable Chem. Eng.* **2014**, *2*, 2658.
[66] L. Huang, W. Liu, J. Wu, Y. Fu, K. Wang, C. Huo, Z. Du, *Tetrahedron Lett.* **2014**, *55*, 2312.
[67] F. Gang, T. Dong, G. Xu, Y. Fu, Z. Du, *Heterocycles* **2015**, *91*, 1964.
[68] N. Pourmohammad, M. M. Heravi, S. Ahmadi, T. Hosseinnejad, *Appl. Organomet. Chem.* **2019**, *33*. https://doi.org/10.1002/aoc.4967
[69] M. Sarvestani, R. Azadi, *Appl. Organomet. Chem.* **2017**, *31*. https://doi.org/10.1002/aoc.3667
[70] G. R. Bardajee, M. Mohammadi, N. Kakavand, *Appl. Organomet. Chem.* **2016**, *30*, 51.
[71] F. Ebrahimpour-Malamir, T. Hosseinnejad, R. Mirsafaei, M. M. Heravi, *Appl. Organomet. Chem.* **2018**, *32*, e3913.
[72] X. Xiong, Z. Tang, Z. Sun, X. Meng, S. Song, Z. Quan, *Appl. Organomet. Chem.* **2018**, *32*, e3946.
[73] W. A. A. Arafa, A. E. A. A. Nayl, *Appl. Organomet. Chem.* **2019**, *33*. https://doi.org/10.1002/aoc.5156
[74] W. Brullot, N. K. Reddy, J. Wouters, V. K. Valev, B. Goderis, J. Vermant, T. Verbiest, *J. Magn. Magn. Mater.* **2012**, *324*, 1919.
[75] C. Hui, C. Shen, J. Tian, L. Bao, H. Ding, C. Li, Y. Tian, X. Shi, H. J. Gao, *Nanoscale* **2011**, *3*, 701.
[76] Y. Xu, Y. Zhou, W. Ma, S. Wang, S. Li, *J. Nanopart. Res.* **2013**, *15*, 1716.
[77] D. Dupont, W. Brullot, M. Bloemen, T. Verbiest, K. Binnemans, *ACS Appl. Mater. Interfaces* **2014**, *6*, 4980.
[78] D. Dupont, J. Luyten, M. Bloemen, T. Verbiest, K. Binnemans, *Ind. Eng. Chem. Res.* **2014**, *53*, 15222.
[79] S. Ranjbar, A. Akbari, N. Edraki, M. Khoshneviszadeh, H. Hemmatian, O. Firuzi, M. Khoshneviszadeh, *Lett. Drug Des. Discov.* **2018**, *15*, 1170.
[80] H. Behbehani, H. M. Ibrahim, *Molecules* **2012**, *17*, 6362.
[81] H. Behbehani, H. Ibrahim, S. Makhseed, *Heterocycles* **2009**, *78*, 3081.
[82] G. Bashiardes, I. Safir, F. Barbot, J. Laduranty, *Tetrahedron Lett.* **2004**, *45*, 1567.

[83] Y. Kitamura, K. Taniguchi, T. Maegawa, Y. Monguchi, Y. Kitade, H. Sajiki, *Heterocycles* **2009**, *77*, 521.
[84] M. Keshavarz, N. Iravani, A. Ghaedi, A. Z. Ahmady, M. Vafaei-Nezhad, S. Karimi, *Springerplus* **2013**, *2*, 1.
[85] C. S. Radatz, L. D. A. Soares, E. R. Vieira, D. Alves, D. Russowsky, P. H. Schneider, *New J. Chem.* **2014**, *38*, 1410.
[86] N. Mukherjee, S. Ahammed, S. Bhadra, B. C. Ranu, *Green Chem.* **2013**, *15*, 389.
[87] F. Alonso, Y. Moglie, G. Radivoy, M. Yus, *Adv. Synth. Catal.* **2010**, *352*, 3208.
[88] V. Bénéteau, A. Olmos, T. Boningari, J. Sommer, P. Pale, *Tetrahedron Lett.* **2010**, *51*, 3673.
[89] R. B. N. Baig, M. N. Nadagouda, R. S. Varma, *Green Chem.* **2014**, *16*, 2122.
[90] M. Mahdavinasab, M. Hamzehloueian, Y. Sarrafi, *Int. J. Biol. Macromol.* **2019**, *138*, 764.

SUPPORTING INFORMATION

Additional supporting information may be found online in the Supporting Information section at the end of this article.

How to cite this article: Darroudi M, Ranjbar S, Esfandiar M, et al. Synthesis of Novel Triazole Incorporated Thiazolone Motifs Having Promising Antityrosinase Activity through Green Nanocatalyst CuI-Fe_3O_4@SiO_2 (TMS-EDTA). *Appl Organomet Chem*. 2020;e5962. https://doi.org/10.1002/aoc.5962